J Mater Sci (2008) 43:7293–7298
DOI 10.1007/s10853-008-2752-5

Decomposition process in a FeAuPd alloy nanostructured by severe plastic deformation

X. Sauvage · A. Chbihi · D. Gunderov · E. V. Belozerov · A. G. Popov

Received: 6 March 2008 / Accepted: 23 May 2008 / Published online: 16 August 2008

Abstract The decomposition process mechanisms have been investigated in a Fe50Au25Pd25 (at.%) alloy processed by severe plastic deformation. Phases were characterized by X-ray diffraction (XRD) and microstructures were observed using transmission electron microscopy (TEM). In the coarse grain alloy homogenized and aged at 450 °C, the bcc α-Fe and fcc AuPd phases nucleate in the fcc supersaturated solid solution and grow by a discontinuous precipitation process resulting in a typical lamellar structure. The grain size of the homogenized FeAuPd alloy was reduced in a range of 50–100 nm by high pressure torsion (HPT). Aging at 450 °C this nanostructure leads to the decomposition of the solid solution into an equi-axed microstructure. The grain growth is very limited during aging and the grain size remains under 100 nm. The combination of two phases with different crystallographic structures (bcc α-Fe and fcc AuPd) and of the nanoscaled grain size gives rise to a significant hardening of the alloy.

Introduction

It is now well demonstrated that severe plastic deformation (SPD) processes are able to produce fully dense bulk nanostructured materials in large quantity. SPD-related techniques like equal channel angular pressing (ECAP) [1], high pressure torsion (HPT) [1] or accumulative roll bounding [2] are usually applied to metals and alloys to produce ultrafine grained structures. The grain size is typically in a range of 100–300 nm for commercially pure metals [1] and could be <20 nm for some specific alloys [3–7]. It is well known that the smaller the grain size, the higher the yield stress (Hall and Petch law [8, 9]); thus, SPD-processed materials usually exhibit a very high strength compared to their coarse grained counterparts. On the other hand, most of them exhibit a low level of ductility [10, 11], with a uniform elongation to failure typically <5%. This lack of ductility is a critical issue and up to now it has strongly limited the application of bulk nanostructured materials produced by SPD as structural components. However, numerous research teams around the world have focused their activities on this issue, and there are now some great hopes to achieve nanostructures with an excellent combination of high strength and good ductility. Thus, Ma and co-authors have recently suggested and also demonstrated that nanoscaled precipitates together with ultrafine grains are a suitable route to reach this goal [12, 13]. The physical reasons could be summarized as follows: in single phase ultrafine grains, dislocations are pinned by grain boundaries and there is no strain hardening because of the lack of dislocation sources. But if there are some nanoscaled precipitates within the grains, they could pin gliding dislocations and contribute to the formation of dislocation sources which give rise to some potential strain hardening and ductility. However, controlling the precipitation of second phase particles in an alloy nanostructured by SPD could be a real challenge. Indeed, during the aging treatment necessary for the nucleation of precipitates, recovery, recrystallization, and grain growth may occur. Moreover, there are so many defects in such nanostructured

X. Sauvage (✉) · A. Chbihi
CNRS UMR 6634, Groupe de Physique des Matériaux, Faculté des Sciences, University of Rouen, Saint-Etienne du Rouvray, BP12, Rouen 76801, France
e-mail: xavier.sauvage@univ-rouen.fr

D. Gunderov
Institute for Physics of Advanced Materials, Ufa State Aviation Technical University, K. Marx 12, Ufa 450000, Russia

E. V. Belozerov · A. G. Popov
Institute of Metal Physics, 18 Kovalevskaya Str., Ekaterinburg 620219, Russia

materials that heterogeneous precipitation along grain boundaries or dislocations is more likely to occur than homogeneous precipitation. The aim of this paper is to bring further knowledge on phase transformation mechanisms in SPD-processed metallic alloys. These features have been investigated in a FeAuPd alloy processed by HPT. The precipitation of the α-Fe bcc phase from the fcc supersaturated solid solution was investigated by X-ray diffraction (XRD) and transmission electron microscopy (TEM). The microstructure of the aged alloy was compared to that of the HPT alloy aged in similar conditions.

Experimental

The alloy investigated in the present study is a Fe50Au25Pd25 (at.%) that was cast from high purity Fe (99.5%) and a Au50Pd50 (at.%) alloy. The as-cast material was homogenized at 900 °C for 6 h in Ar atmosphere and subsequently quenched in ice brine. A part of the homogenized alloy was aged for 30 h at 450 °C, and the other part was used for SPD experiments. The material was processed by HPT at room temperature under a pressure of 6 GPa. HPT samples (discs 10 mm in diameter and with a thickness of 0.3 mm) were subjected to 5 revolutions (0.2 rpm) and then aged for 30 h at 450 °C.

Crystallographic phases were characterized by XRD. Spectra were recorded with a Brucker D8 system in Bragg–Brentano θ–2θ geometry. The X-ray generator was equipped with a Co anticathode, using Co (Kα) radiation ($\lambda = 0.17909$ nm). The measurements were performed so that the out-of-plane component was the torsion axis of the sample processed by HPT.

Microstructures were characterized by TEM. Observations were performed with a JEOL 2000FX microscope operating at 200 kV. TEM samples were prepared by ion milling (PIPS-GATAN 691, 3 kV, beam angle 4°, 300 K). Samples with a diameter of 3 mm were cut in the discs processed by HPT at a distance of 3 mm from the disc center (corresponding to a shear strain of about $\gamma \approx 300$). The TEM investigations were performed with the electron beam parallel to the torsion axis.

The Vickers microhardness of the alloy was measured with a BUEHLER Micromet 2003 machine, using a 300 g load (2.94 N).

Results and discussions

Decomposition process in the coarse grained FeAuPd alloy

The XRD spectrum of the homogenized FeAuPd alloy is displayed in Fig. 1a. It clearly shows that the probed sample contains only one fcc disordered phase with all elements in solid solution. The lattice parameter of this phase calculated from these data is 0.510 nm (±0.001). After aging at 450 °C for 30 h (Fig. 1b), an additional phase is detected indicating that the solid solution is decomposed. The new peak corresponds to the (110) diffraction peak of the bcc α-Fe phase (lattice parameter 0.287 nm ± 0.001). The TEM bright field image (Fig. 1c) clearly shows the two-phase microstructure. Obviously

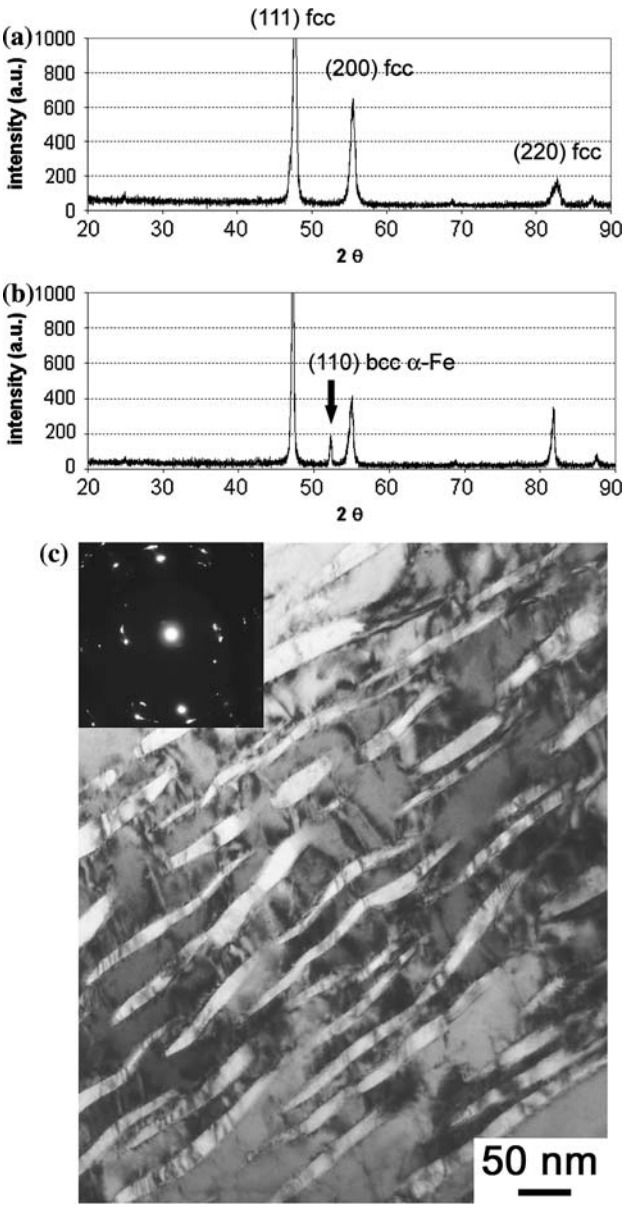

Fig. 1 (**a**) X-ray diffraction spectrum of the homogenized FeAuPd alloy showing that there is a single fcc phase. (**b**) X-ray diffraction of the non-deformed FeAuPd alloy after aging at 450 °C for 30 h showing that the α-Fe bcc has nucleated. (**c**) TEM bright field image and corresponding SAED pattern (aperture size 2 μm) showing the microstructure of non-deformed FeAuPd alloy after aging at 450 °C for 30 h

some discontinuous precipitation occurred resulting in a typical lamellar structure [14]. In agreement with XRD data, the bright lamellae have a bcc crystallographic structure, and using X-ray energy dispersive spectroscopy (EDS), only Fe was detected (data not shown here). These bcc lamellae are embedded in the disordered fcc AuPd matrix (Fe was not detected in this phase by EDS). The lamellae thickness is in the range of 10–30 nm, while their length is in the range of 50–300 nm. The lamellae have a wavy shape and it is therefore difficult to fully image one of them orientated perpendicular to the electron beam. Anyway, some attempts were carried out and a lamella imaged with such an orientation is shown in Fig. 2. From such images, the average width of lamellae (third dimension) was estimated to be in a range of 50–100 nm. It is interesting to note that the nucleation and growth of these lamellae induce a significant hardening of the alloy, from 2 GPa after the homogenization treatment, up to 3.7 GPa after aging (see Table 1).

Microstructure of the FeAuPd alloy processed by HPT

The XRD spectrum of the homogenized FeAuPd alloy processed by HPT is displayed in Fig. 3a. Compared to the non-deformed alloy (Fig. 1a), there is a significant broadening of the diffraction peaks. This feature is commonly observed in SPD metals and results from grain size reduction and internal stresses [1]. As shown in the TEM bright field image, the grain size is indeed very small after HPT (Fig. 4). The selected area electron diffraction pattern recorded with an aperture of only 2 μm exhibits Debye–Scherrer rings typical of nanocrystalline structures with high angle grain boundaries. The dark field image (Fig. 4b) obtained by selecting a part of the more intense ring clearly shows that the grain size is in the range of 50–100 nm. As a result of this nanostructuration, the hardness has significantly increased up to 3.4 GPa, thus reaching a value close

Table 1 Microhardness of the FeAuPd alloy after homogenization, homogenization + aging at 450 °C for 30 h, homogenization + 5 revolutions by HPT, homogenization + 5 revolutions by HPT + aging at 450 °C for 30 h

	Homogenized	Aged	HPT	HPT + aged
HV (GPa)	2 ± 0.1	3.7 ± 0.1	3.4 ± 0.1	4.7 ± 0.1

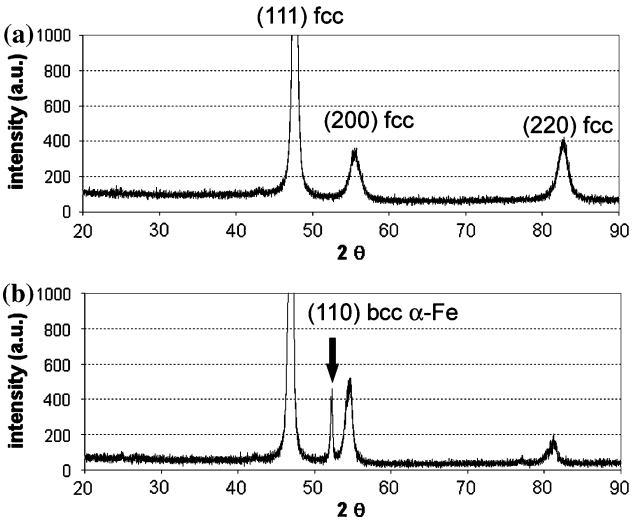

Fig. 3 (**a**) X-ray diffraction spectrum of the homogenized FeAuPd alloy after HPT processing showing that there is a single fcc phase. (**b**) X-ray diffraction of the homogenized FeAuPd alloy after HPT processing followed by subsequent aging at 450 °C for 30 h showing that the α-Fe bcc phase has nucleated

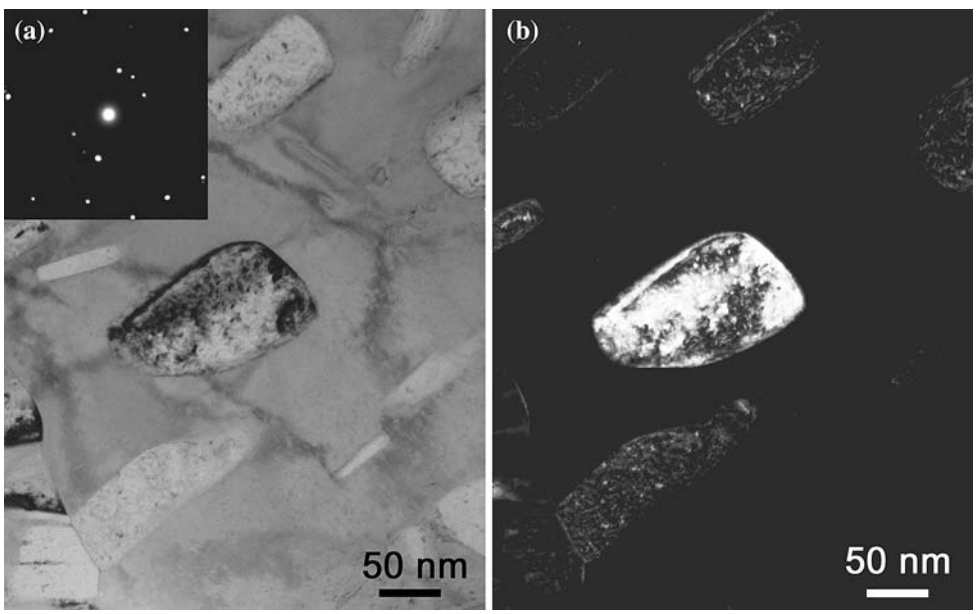

Fig. 2 (**a**) High magnification TEM bright field image and corresponding SAED pattern (aperture size 2 μm) showing the cross section of a rod shaped bcc α-Fe precipitate in the non-deformed FeAuPd alloy after aging at 450 °C for 30 h. (**b**) Corresponding dark field image where only the α-Fe precipitate is imaged

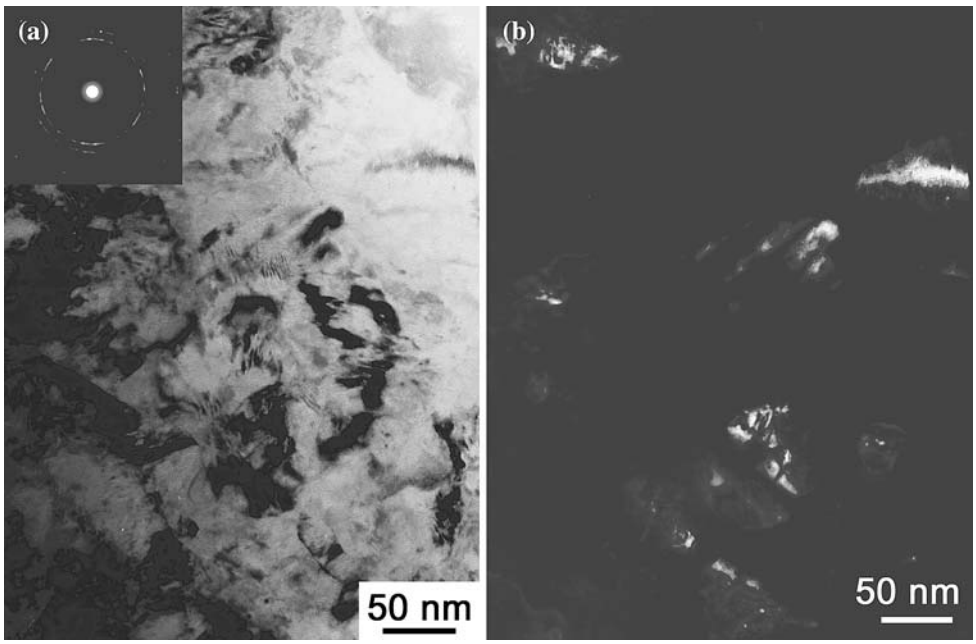

Fig. 4 (**a**) TEM bright field image and corresponding SAED pattern (aperture size 2 μm) of the microstructure of the homogenized FeAuPd alloy processed by HPT. (**b**) Corresponding dark field image showing few isolated fcc grains

to that obtained after aging and precipitation in the non-deformed material (Table 1). Even if the level of deformation is much higher in the outer part of the HPT disc [1], it is worth noticing that the hardness does not fluctuate significantly along the diameter of the sample.

Decomposition process in the nanocrystalline FeAuPd alloy

The FeAuPd alloy processed by HPT was aged at 450 °C for 30 h and the XRD spectrum (Fig. 3b) does not show any significant difference compared to the non-deformed alloy (Fig. 1b). Similarly, decomposition occurred during the aging treatment and the fcc matrix is detected together with the bcc α-Fe phase. However, as exhibited on the bright field TEM picture (Fig. 5a), the microstructure is very different. The grain size did not change significantly during aging (in a range of 70–100 nm) and obviously bcc α-Fe grains that have nucleated and grew are not lamella shaped. The high magnification TEM bright field image of Fig. 5b displays a large bcc α-Fe grain (brightly imaged). This large grain was selected because smaller grains were difficult to image.

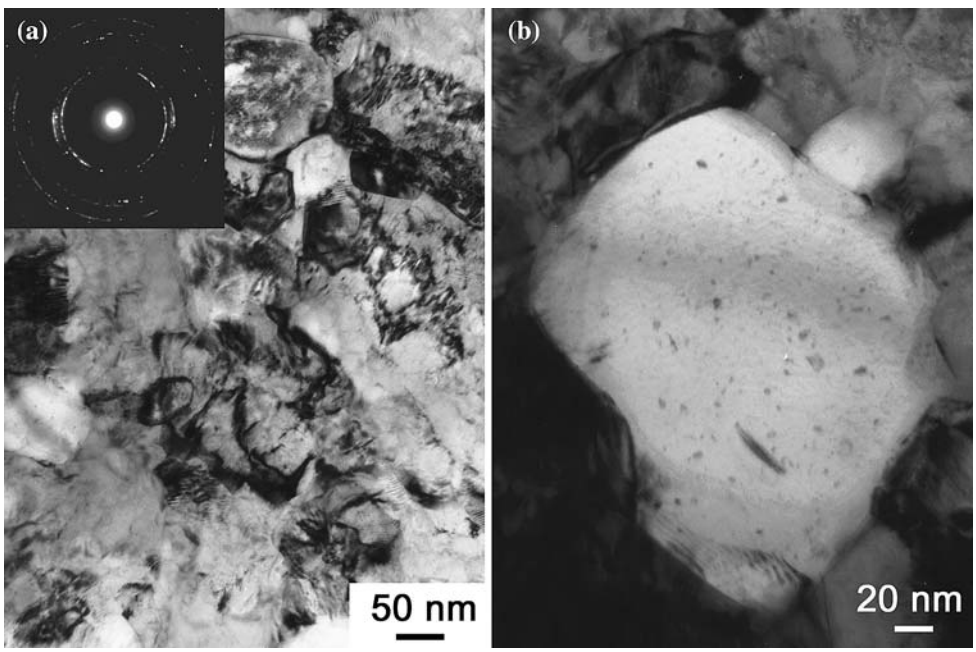

Fig. 5 (**a**) TEM bright field image and corresponding SAED pattern (aperture size 2 μm) of the microstructure of the homogenized FeAuPd alloy processed by HPT and subsequently aged at 450 °C for 30 h. (**b**) High magnification TEM bright field image of an equi-axed bcc α-Fe grain that has precipitated within the nanostructure

Anyway, it shows that bcc α-Fe grains are nanoscaled and almost equi-axed. Thus, it seems that during the aging treatment heterogeneous nucleation occurred along grain boundaries of the nanocrystalline fcc solid solution produced by SPD. It is interesting to note that the precipitation of this second phase induces a significant increase of the hardness up to 4.7 GPa, which is 1 GPa higher than the hardness of the non-deformed material after similar aging treatment (Table 1). As noticed for the HPT sample, the hardness was fairly constant across the diameter of the sample.

Discussion

The decomposition process in the coarse grained FeAuPd alloy is clearly a discontinuous precipitation regime resulting in a typical lamellar microstructure thanks to the redistribution of Au, Pd, and Fe atoms (Fig. 6a). The high volume fraction of lamella shaped bcc α-Fe precipitates provides some efficient obstacles for dislocation glide and this leads to a significant increase of the hardness (Table 1). In the nanostructured alloy, the situation is very different because there are numerous high angle grain boundaries (Fig. 4) that could act as nucleation sites. Moreover, as schematically represented in Fig. 6b, the grain size is close to the typical length scale of the lamellar structure that grows in the coarse grain alloy. Thus, theoretically, if a bcc α-Fe lamella grows from one grain boundary, it would simply split a grain. It seems however, that this situation never occurs since only equi-axed grains were observed by TEM (Fig. 5). This feature could be attributed to the higher atomic mobility of solute elements along grain boundaries: once a grain nucleates on a grain boundary, it is simply fed by atoms migrating along this grain boundary (Fig. 6c). This scenario is completely different from the decomposition process that occurs in the coarse grain material, and is the consequence of the nanoscaled structure that was achieved by SPD. It is also interesting to note that there is no significant grain growth during the aging treatment (Figs. 4, 5). This indicates that even if there is a significant atomic mobility (otherwise precipitation would not occurr), a small grain can be kept upon aging and precipitation. In the present case, there is a competition between decomposition (bcc α-Fe and fcc AuPd grain growth) and coarsening to reduce the interfacial energy. Since the microstructure is a mixture of two phases with nanoscaled grains, grain boundaries pin each other and cannot migrate easily. Therefore, after aging, even if the microstructure has completely changed (full redistribution of Fe atoms), the small grain size was kept. Finally, this combination of nanoscaled grains together with a mixture of two phases with different crystallographic structures gives rise to a much higher hardness than the non-deformed alloy (Table 1).

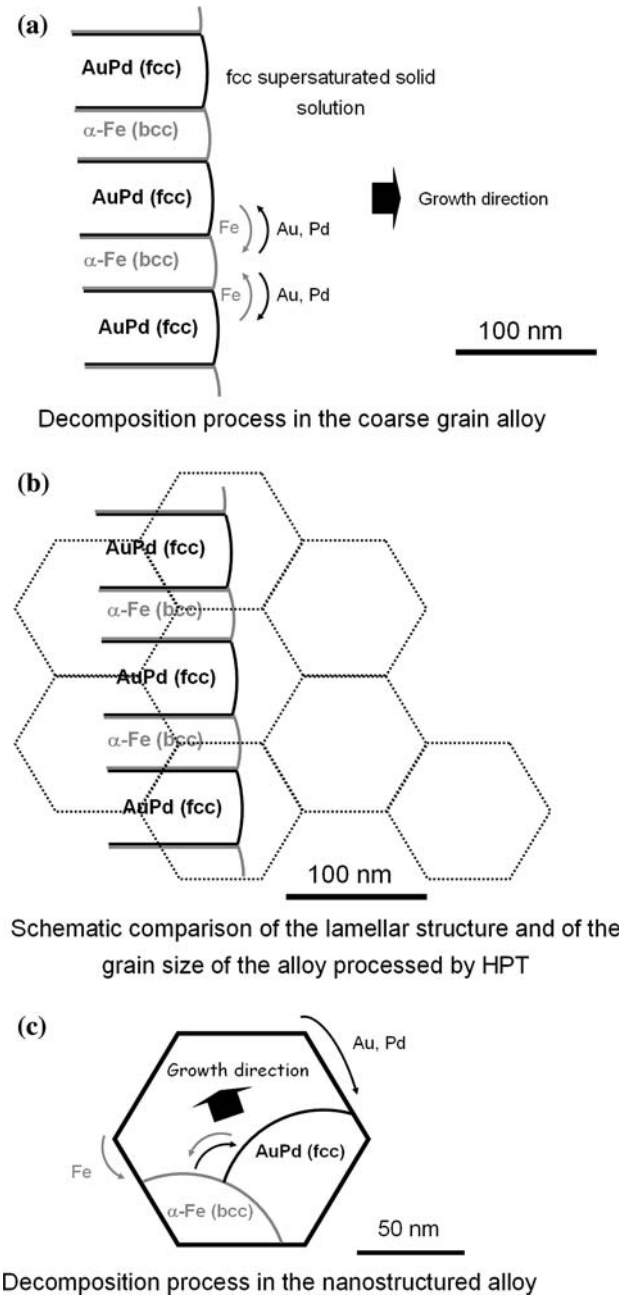

Fig. 6 (**a**) Schematic representation of the decomposition process in the coarse grained alloy resulting in a lamellar structure; (**b**) comparison of the grain size after HPT with the typical length scale of the lamellar structure; (**c**) schematic representation of the decomposition process in the nanostructured alloy resulting in an equi-axed structure

Conclusions

1. In the coarse grain Fe50Au25Pd25 alloy homogenized at 900 °C, the fcc solid solution is transformed into a two phase microstructure during aging at 450 °C (fcc AuPd and bcc α-Fe). This is a lamellar structure resulting from a discontinuous precipitation mechanism.

2. The grain size of the Fe50Au25Pd25 alloy homogenized at 900 °C was reduced in the range of 50–100 nm by HPT. In this nanostructured alloy, the decomposition process is different and does not result in a lamellar structure.
3. The alloy processed by HPT and subsequently aged at 450 °C is completely phase separated but grains do not significantly grow. The combination of two phases with different crystallographic structures and of the nanoscaled grain size gives rise to a strong hardening.
4. Thus, this work demonstrates that it is possible to combine precipitation hardening together with nanoscaled grains.

References

1. Valiev RZ, Islamgaliev RK, Alexandrov IV (2000) Prog Mater Sci 45:103
2. Saito S, Tsuji N, Utsunomiya H, Sakai T, Hong RG (1998) Scr Mater 39:1221
3. Sauvage X, Ivanisenko Y (2007) J Mater Sci 42:1615
4. Korznikov AV, Dimitrov O, Korznikova GF, Dallas JP, Quivy A, Valiev RZ, Mukherjee A (1999) Nanostruct Mater 11:17
5. Sauvage X, Pippan R (2005) Mater Sci Eng A 410–411:345
6. Sabirov I, Pippan R (2005) Scr Mater 52:1293
7. Sauvage X, Jessner P, Vurpillot F, Pippan R (2008) Scr Mater 58:1125
8. Hall EO (1951) Proc Phys Soc B 64:747
9. Petch NJ (1953) J Iron Steel Inst 173:25
10. Valiev R (2004) Nat Mater 3:511
11. Ma E (2003) Nat Mater 2:7
12. Cheng S, Zhao YH, Zhu YT, Ma E (2007) Acta Mater 55:5822
13. Ma E (2006) JOM 58(4):49
14. Turnbull D (1955) Acta Metall 3:55